PII S0016-7037(00)00780-3

Temperature dependence of goethite dissolution promoted by trihydroxamate siderophores

Claudio Cocozza,[1] Calvin C. G. Tsao,[2] Sing-Foong Cheah,[2] Stephan M. Kraemer,[3] Kenneth N. Raymond,[4]
Teodoro M. Miano,[1] and Garrison Sposito[2,*]

[1]Dipartimento di Biologia e Chimica Agro-Forestale e Ambientale, Universitá degli Studi di Bari, 70126 Bari, Italy
[2]Division of Ecosystem Sciences, University of California, Berkeley, CA 94720-3110, USA
[3]Institute of Terrestrial Ecology, ETH-Zürich, CH-8952, Schlieren, Switzerland
[4]Department of Chemistry, University of California, Berkeley, CA 94720-1460, USA

Abstract—This article reports an investigation of the temperature dependence of goethite dissolution kinetics in the presence of desferrioxamine B (DFO-B), a trihydroxamate siderophore, and its acetyl derivative, desferrioxamine D1 (DFO-D1). At 25 and 40°C, DFO-D1 dissolved goethite at twice the rate of DFO-B, whereas at 55°C, the behavior of the two ligands was almost the same. Increasing the temperature from 25 to 55°C caused little or no significant change in DFO-B or DFO-D1 adsorption by goethite. A pseudo–first-order rate coefficient for dissolution, calculated as the ratio of the mass-normalized dissolution rate coefficient to the surface excess of siderophore, was approximately the same at 25 and 40°C for both siderophores. At 55°C, however, this rate coefficient for DFO-D1 was about half that for DFO-B. Analysis of the temperature dependence of the mass-normalized dissolution rate coefficient via the Arrhenius equation led to an apparent activation energy that was larger for DFO-B than for DFO-D1, but much smaller than that reported for the proton-promoted dissolution of goethite. A compensation law was found to relate the pre-exponential factor to the apparent activation energy in the Arrhenius equation, in agreement with what has been noted for the proton-promoted dissolution of oxide minerals and for the complexation of Fe^{3+} by DFO-B and simple hydroxamate ligands in aqueous solution. Analysis of these results suggested that the siderophores adsorb on goethite with a only single hydroxamate group in bidentate ligation with an Fe(III) center. *Copyright © 2002 Elsevier Science Ltd*

1. INTRODUCTION

The importance of microbial siderophores [$\sigma\iota\delta\eta\rho o\varsigma$ (iron) + $\phi\acute{\epsilon}\rho\omega$ (carry)] in mineral weathering reactions has long been recognized (see, e.g., Cornell and Schwertmann, 1996), but it is only very recently that the geochemistry of these Fe(III)-specific ligands has been investigated quantitatively. Kalinowski et al. (2000) catalogued the few available data on siderophore-promoted mineral dissolution kinetics, noting a relatively modest rate enhancement by siderophores over proton-promoted dissolution under the same conditions. They noted also that a saturation effect exists when dissolution rates are measured as a function of increasing siderophore concentration, which supports the concept of Stumm et al. (1987), that surface complexation of a ligand is a precursor to ligand-promoted mineral dissolution.

Most geochemical studies of siderophore-promoted mineral dissolution have utilized the common trihydroxamate siderophore, desferrioxamine B (DFO-B, Fig. 1), which possesses three hydroxamate functional groups, each comprising a carbonyl adjacent to a hydroxylamine. The aqueous solution chemistry of this siderophore has been investigated extensively, with a number of its thermodynamics and kinetic parameters now reported (Biruš et al., 1988; Crumbliss, 1991; Albrecht-Gary and Crumbliss, 1998). Analyzing their experiments on the DFO-promoted dissolution kinetics of goethite (α-FeOOH), Kraemer et al. (1999) drew on this kind of information to speculate that the three hydroxamate groups in DFO-B might

coordinate to surface Fe(III) centers independently while promoting dissolution. Liermann et al. (2000) observed an approximately square-root dependence on DFO-B concentration for the Fe release rate from hornblende, leading them to conclude that DFO-B adsorption is necessary to mineral dissolution. Holmén and Casey (1996, 1998) and Holmén et al. (1997) have added mechanistic details to this picture in their careful investigations of the dissolution of goethite promoted by acetohydroxamic acid [$CH_3COHNOH$, aHA], a simple monohydroxamate ligand. They concluded that the aHA hydroxamate group coordinates to a surface Fe(III) center on the mineral in much the same way as in aqueous solution (i.e., bidentate ligation), but does so with the greater impact of vicinal atoms in the mineral, as compared with solvating water molecules in aqueous solution, on the distribution of electron density within the surface complex.

All previous studies of siderophore-promoted dissolution have been performed at ambient temperature. In this article, we report the first investigation of the temperature dependence of both ligand adsorption and mineral dissolution kinetics for goethite in the presence of the two important hydroxamate siderophores, DFO-B and DFO-D1 (Fig. 1), the latter of which is an uncharged acetyl derivative of DFO-B (van der Helm et al., 1987). The objectives of our research were to determine quantitatively the effect of increasing temperature on the processes underlying goethite weathering by trihydroxamate siderophores and to elucidate further the mechanisms of siderophore-promoted goethite dissolution through an analysis of temperature-dependent kinetics along conventional geochemical lines (Lasaga, 1998), while informed by comparable data

---

* Author to whom correspondence should be addressed (gsposito@nature.berkeley.edu).
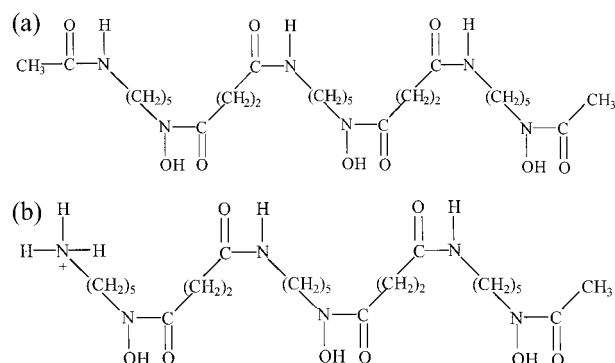
Fig. 1. Molecular structures of (a) DFO-D1 and (b) DFO-B.

for the aqueous solution reactions of DFO-B (Biruš et al., 1988; Crumbliss, 1991).

2. MATERIALS AND METHODS

2.1. Materials

Goethite was synthesized following the method of Schwertmann and Cornell (1991). Briefly, 180 mL of 5 mol/L KOH solution was added rapidly with stirring to 100 mL of 1 mol/L $Fe(NO_3)_3$ solution in a 2-L polyethylene flask. The resulting suspension was then brought to a 2-L total volume with high-purity 18 $M\Omega$ cm^{-1} water (Milli-Q Plus, Millipore) and heated at 70°C for 60 h. Next, the precipitated product was centrifuged, washed with high-purity water, and freeze-dried. Powder X-ray diffraction and Fourier transform infrared spectroscopy confirmed that the synthesized solid was indeed goethite. The specific surface area of the sample was not determined but should be similar to that of the goethite sample prepared in identical fashion by Kraemer et al. (1999), 35 ± 3 m^2/g.

The sample of DFO-B used was the mesylate salt $[C_{25}H_{46}N_5O_8NH_3^+(CH_3SO_3^-)]$ produced by Ciba-Geigy (Desferal) and received as a gift from the Salutar Corporation. The sample of DFO-D1 ($C_{27}H_{50}N_6O_9$) used was prepared from DFO-B by per-acetylation in methanol as described by Kraemer et al. (1999).

2.2. Dissolution Experiments

Goethite dissolution kinetics were measured at pH 6.5 in batch reactors open to the atmosphere. The pH value was selected to ensure negligible proton- or hydroxide ion–promoted dissolution and particle coagulation during the 350-h reaction period. The solids concentration was 0.5 g/L at 25 and 40°C; 0.1 g/L was used at 55°C. The lower solids concentration was selected so as to maintain far-from-equilibrium conditions throughout the dissolution experiment, given the expected high dissolution rate at 55°C. The background electrolyte solution was 0.01 mol/L $NaClO_4$ mixed with 5 mM MOPS pH buffer ($C_7H_{15}NSO_4$), a weakly complexing tertiary amine (Yu et al., 1997).

In each dissolution experiment, goethite was placed in wide-mouthed polypropylene bottles wrapped with Al foil and suspended in the background electrolyte solution by ultrasonication for 1 min. Then DFO-B or DFO-D1 solution was added to achieve an initial concentration of 240 μM, and pH was adjusted to 6.5 with 0.1 mol/L NaOH or $HClO_4$. Background electrolyte solution was added to make the total sample mass 200 g. Sample stirring was accomplished by floating stir bars, and constant temperature (± 1°C) was maintained by immersion in a thermally controlled water bath. Aliquots taken periodically over 350 h reaction time were filtered with 0.05-μm syringe filters (MF-Millipore). The first 3 mL of filtrate was discarded; the second 5 mL was retained for pH measurement, and 10 mL of filtrate was acidified to approximately pH 1.5 with concentrated perchloric acid. This last aliquot was stored under refrigeration for no more than 1 week before Fe analysis with a Thermal Jarrel-Ash ICP-AES unit reading emission at 238.2 nm.

2.3. Adsorption Experiments

Adsorption of DFO-B and DFO-D1 on goethite was measured in batch reactors, open to the atmosphere, at the high solids concentration of 20 g/L, selected because DFO-B and DFO-D1 adsorption on goethite is relatively low at submillimolar initial concentrations (Kraemer et al., 1999). Because far-from-equilibrium ligand-promoted dissolution rates are expected to increase with the surface excess of the ligand (Stumm et al., 1987), a disadvantage of this arrangement is significant Fe release and a concomitant decrease in free siderophore concentration, necessitating a short reaction time. On the other hand, a short reaction time is consistent with measuring the rapid component of ligand adsorption, free from the effects of the subsequent slow detachment of Fe(III)-ligand complexes into aqueous solution. Preliminary adsorption kinetics experiments involving 30, 60, 180, and 300 min reaction time (data not shown) indicated that the DFO-B adsorption rate dropped sharply after 60 min and therefore that 60 min was an optimal reaction period to achieve adsorption without significant dissolution.

Adsorption was investigated at pH 6.5 in 0.01 mol/L $NaClO_4$ solution that contained 5 mM MOPS buffer. All samples were prepared in duplicate. Blanks (i.e., samples without goethite) were prepared to investigate adsorption to container walls and filters. In these batch studies, goethite and background electrolyte with buffer were placed in 30 mL amber HDPE bottles wrapped with Al foil. Predetermined amounts of 1 mol/L NaOH were added to reach the desired pH value. The sample bottle was filled with electrolyte solution to a final mass of 20 g and placed in a temperature-controlled water bath at 25, 40, or 55°C. Then DFO-B or DFO-D1 stock solution was added to give an initial concentration of 300 μM.

For each siderophore at each reaction temperature, aliquots were taken from the duplicate samples and blanks, then filtered through 0.05-μm Millipore membrane filters. A 3-mL portion from each filtrate was used for pH measurement. The remaining filtrate was separated into two 5-mL aliquots that were acidified to pH 1.5 to 1.7 with concentrated perchloric acid. One aliquot of each pair then received 167 μL of $Fe(ClO_4)_3$ stock solution (15 mM or 18 mM $Fe(ClO_4)_3$ for DFO-B or DFO-D1, respectively).

Aliquots from the adsorption experiments were analyzed for siderophore concentration following the Fe(III) chelometric method of Solinas (1994), but with solid-phase separation by filtration instead of centrifugation. The absorbance of all sample and blank filtrates, both with and without added Fe, was measured at 441 nm (DFO-B) or 474.5 nm (DFO-D1). The net absorbance of the blank-corrected sample aliquot to which Fe stock solution had been added was attributed to the concentration of siderophore not adsorbed. The surface excess of siderophore (μmol/g) was then calculated on dividing the corresponding concentration loss (300 μM minus the sample concentration) by the solids concentration. The net absorbance of the blank-corrected sample aliquot to which Fe stock solution had not been added was used to monitor Fe released by goethite dissolution during the adsorption reaction. The concentration of dissolved Fe released after the 1-h adsorption experiment increased monotonically with temperature, averaging 2.5, 36, and 109 μM for DFO-B and 20, 21, and 49 μM for DFO-D1 at 25, 40, and 55°C, respectively.

Standards for the absorbance measurements were prepared by adding 1 mL Fe stock solution to solutions of 0, 60, 120, 180, 240, and 300 μM siderophore in 0.01 mol/L $NaClO_4$ and acidifying to pH 1.5 with $HClO_4$. Absorbance was read on a Shimadzu UV 160 spectrophotometer with baseline correction. Proton activity was measured with a Ross combination electrode calibrated at pH 4.0, 7.0, and 10.0, with temperature correction.

3. RESULTS

Figures 2 and 3 show Fe release kinetics for goethite in the presence of the two siderophores at 240 μM initial concentration. As observed also by Holmén and Casey (1996) for aHA, Fe release after 50 h followed zero-order kinetics, and the Fe concentrations depended linearly on time (Table 1), which is typical for dissolution reactions under far-from-equilibrium conditions (Stumm et al., 1987; Sposito, 1994; Lasaga, 1998).
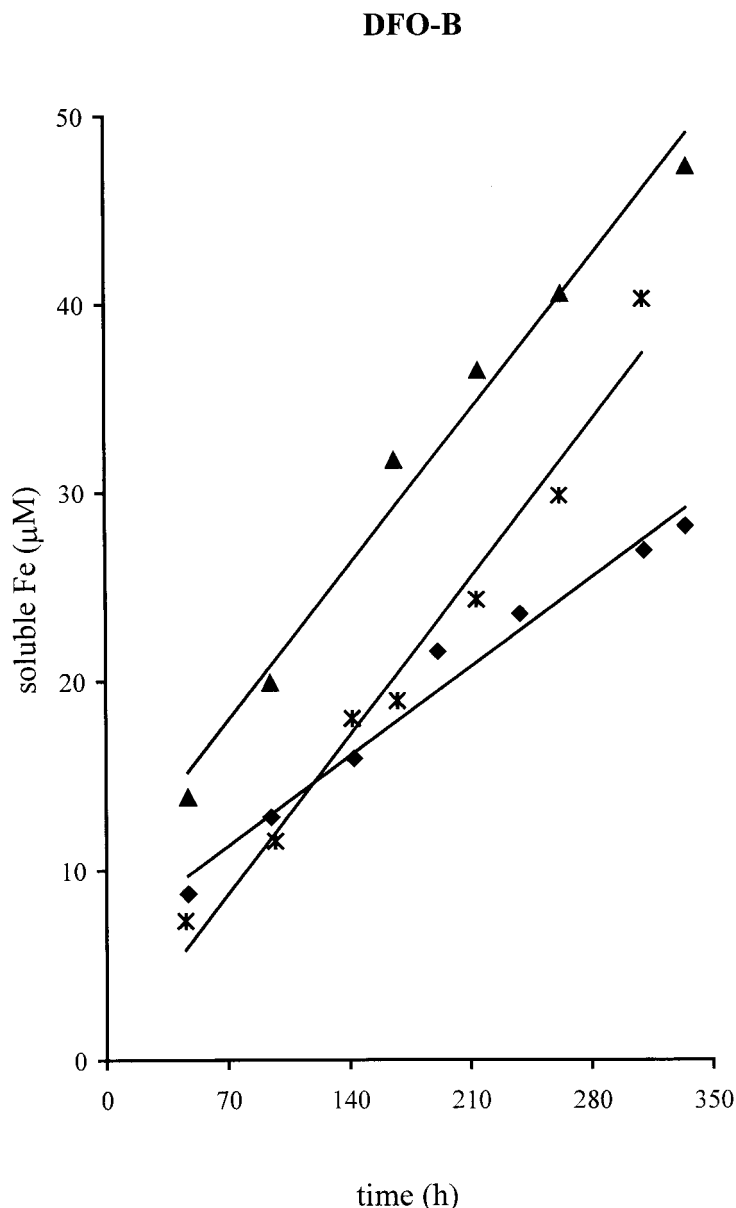
DFO-B

Fig. 2. Iron release by goethite in presence of DFO-B at 25°C (diamonds), 40°C (triangles), and 55°C (asterisks). The lines through the data are linear regressions (Table 1). Initial siderophore concentration: 240 μM; solid concentration: 0.5 g/L at 25 and 40°C, 0.1 g/L at 55°C; pH 6.5

The zero-order rate coefficient for Fe release is then equal to the slope of the regression-line equations in column 3 of Table 1. Increasing the temperature from 25 to 40°C caused a significant ($p = 0.05$) increase in the slopes of the linear fits for both siderophores. The same was not true for increasing temperature from 40 to 55°C, but this is an effect of the much lower solids concentration used at the higher temperature. It is notable that Fe release in the presence of DFO-D1 was greater than that in the presence of DFO-B at 25 and 40°C, whereas at 55°C, it was the same for both siderophores within experimental precision.

The zero-order rate coefficient for dissolution reactions far from equilibrium is commonly assumed to be proportional to either the mass or the specific surface area of the dissolving solid (Zinder et al., 1986; Stumm et al., 1987; Lasaga, 1998). Brantley and Chen (1995) have reviewed the problematic issue of surface area normalization of mineral dissolution rates, leading us to choose mass normalization instead. Thus, a mass-normalized rate coefficient for dissolution (μmol g^{-1} h^{-1}) was calculated as the slope of the Fe release curve (Figs. 2 and 3) divided by the solids concentration. Values of the rate coefficient computed in this way are listed in the fourth column of Table 1. At 25 and 40°C, this dissolution rate coefficient is about twice as large for DFO-D1 as for DFO-B, whereas at 55°C, it is the same for both siderophores. For DFO-B, the rate coefficient is five times larger at 55°C than at 40°C. The mass-normalized dissolution rate coefficient for DFO-D1 ap-
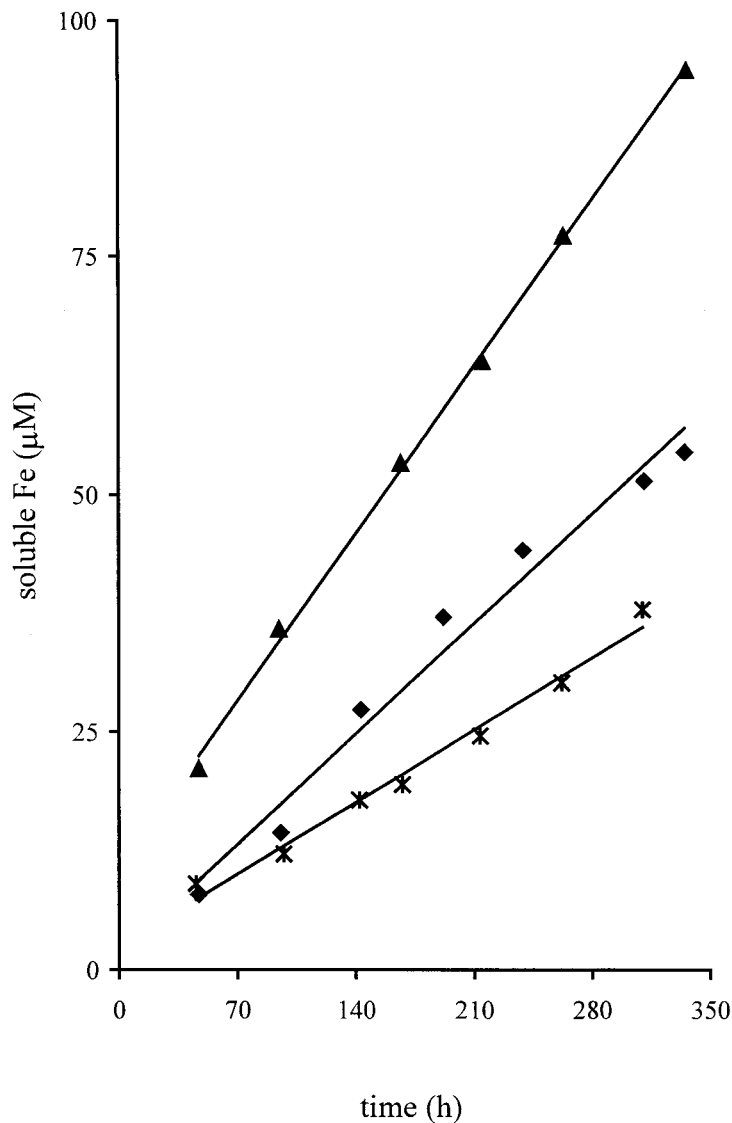
DFO-D1

Fig. 3. Iron release by goethite in presence of DFO-D1 at 25°C (diamonds), 40°C (triangles), and 55°C (asterisks). The lines through the data are linear regressions (Table 1). Initial siderophore concentration: 240 μM; solid concentration: 0.5 g/L at 25 and 40°C, 0.1 g/L at 55°C; pH 6.5.

proximately doubles for every 15°C increase in temperature between 25 and 55°C, whereas that for DFO-B exhibits this behavior only between 25 and 40°C.

Kraemer et al. (1999) reported mass-normalized dissolution rates for goethite dissolution in the presence of DFO-B or DFO-D1 at 25°C that are substantially smaller than the values given in Table 1. Although their experimental conditions were the same as used in the present study, their sample of goethite was not. Cornell and Schwertmann (1996) have noted that large differences exist among the proton-promoted dissolution rates published for goethite, which vary over orders of magnitude without correlation to specific surface area, crystallite length, or isomorphic substitution. They cite as the likely cause of this

variability the strong influence of crystallite morphology, which changes substantially with conditions of mineral formation and pretreatment. Similarly, Eick et al. (1999) reported oxalate-promoted dissolution rates for goethite that were an order of magnitude smaller than those reported by Zinder et al. (1986) under the same reactor experimental conditions. Eick et al. (1999) noted that their goethite sample was freeze-dried after preparation and used without preconditioning, whereas that of Zinder et al. (1986) was pretreated in HF and preconditioned in oxalate solution for 3 d.

Table 2 lists values of the surface excess of DFO-B and DFO-D1 at 25, 40, and 55°C on goethite at pH 6.5 and 300 μM initial siderophore concentration. The supernatant solution sid-

Table 1. Linear regression equations and mass-normalized zero-order dissolution rate coefficient based on the Fe release data in Figs. 2 and 3.

Siderophore[a]	Temperature (°C)	Regression equation[b]	Rate coefficient (μmol/g/h)
DFO-B	25	$Y = (0.067 \pm 0.012)X + (6.6 \pm 2.6)$[c]	0.135 ± 0.024[c]
	40	$Y = (0.117 \pm 0.022)X + (9.7 \pm 4.6)$	0.234 ± 0.044
	55	$Y = (0.119 \pm 0.022)X + (0.4 \pm 4.4)$	1.191 ± 0.222
DFO-D1	25	$Y = (0.165 \pm 0.030)X + (1.6 \pm 6.6)$	0.330 ± 0.060
	40	$Y = (0.251 \pm 0.013)X + (10.7 \pm 2.8)$	0.503 ± 0.026
	55	$Y = (0.108 \pm 0.015)X + (2.4 \pm 3.1)$	1.084 ± 0.156

[a] Initial siderophore concentration = 240 μM.
[b] Y = soluble Fe(μM), X = time (h)
[c] Value ± 95% confidence interval ($p = 0.05$)

erophore concentrations after equilibration ranged from 176 to 274 μM, all of which should be sufficient for maximal adsorption at pH 6.5 (Kraemer et al., 1999). For DFO-B, there was no significant change in surface excess as the temperature was increased from 25 to 55°C, whereas for DFO-D1, a small increase occurred between 25 and 40°C.

Stumm et al. (1987) have proposed that ligand-promoted mineral dissolution kinetics far from equilibrium can be characterized by a pseudo–first-order rate coefficient obtained as the ratio of the mass-normalized (or surface area–normalized) dissolution rate coefficient to the surface excess of the ligand promoting dissolution (h^{-1}). For example, Holmén and Casey (1998) calculated a pseudo–first-order rate coefficient equal to $0.073 \ h^{-1}$ on the basis of their dissolution rate data for goethite at 25°C in the presence of 10 mM aHA at pH 4.5 to 9 (fig. 5 in Holmén and Casey, 1996) combined with their adsorption edge data for aHA on goethite (fig. 7a in Holmén and Casey, 1996) obtained over the same pH range, but with varying total aHA concentration (0.1 to 1 mM aHA). In the present study, we have combined the dissolution rate data in Table 1 with the surface excess data in Table 2 to calculate a pseudo–first-order rate coefficient for dissolution (column 4 of Table 2). Although the pH and total siderophore concentration for the two data sets are comparable, the solids concentrations differed substantially. Thus, we assume that this difference does not affect the surface excess significantly.

At 25 and 40°C, the pseudo–first-order rate coefficient is the same for both siderophores, within experimental precision, and is independent of temperature. The pseudo–first-order rate coefficient that can be calculated with the dissolution rate and

adsorption data of Kraemer et al. (1999) for DFO-D1 at 25°C ($0.05 \ h^{-1}$) is consistent with the results in Table 2, but that reported for DFO-B is much lower ($0.01 \ h^{-1}$). The data obtained in the present study suggest that, in the temperature range 25 to 40°C, the pseudo–first-order rate coefficient for the dissolution of goethite promoted by the two trihydroxamate siderophores has a temperature dependence that is essentially the same as that of adsorption. At 55°C, however, the pseudo–first-order rate coefficient increases markedly and is no longer the same for the two siderophores, that for DFO-D1 falling to half the value for DFO-B. Therefore, surface excess, as measured in our experiments, was not the sole determinant of the temperature dependence of the rate of goethite dissolution promoted by the siderophores. This finding complements the suite of results at fixed temperature, in which proportionality exists between a ligand-promoted dissolution rate and a ligand surface excess (see, e.g., Stumm and Furrer, 1987).

4. DISCUSSION

The data in Tables 1 and 2 indicate that at pH 6.5, DFO-D1 adsorbs more strongly and promotes dissolution more effectively than DFO-B at 25 and 40°C, an effect also noted by Kraemer et al. (1999) at the lower temperature. This difference was attributed by them to electrostatic repulsion of the cationic DFO-B ($pK_a \approx 8.5$; see row 1 in Table 3) by the positively charged goethite surface at pH 6.5 (p.z.n.p.c. = 8.1 [25°C], 8.3 [40°C], 7.9 [55°C]; Rodda et al., 1993). In contrast, DFO-D1 is a neutral species and therefore would not be repelled from the goethite surface.

Table 2. Surface excess values for DFO-B and DFO-D1, together with the associated pseudo–first-order rate coefficients for goethite dissolution (pH 6.5).

Siderophore[a]	Temperature (°C)	Surface excess (μmol/g)	Pseudo–first-order rate coefficient (h^{-1})
DFO-B	25	2.99 ± 0.37[b]	0.05 ± 0.01[b]
	40	3.18 ± 0.09	0.07 ± 0.01
	55	3.64 ± 0.47	0.33 ± 0.07
DFO-D1	25	5.49 ± 0.19	0.06 ± 0.01
	40	7.15 ± 0.71	0.07 ± 0.01
	55	6.86 ± 0.67	0.16 ± 0.03

[a] Initial siderophore concentration = 300 μM.
[b] Measured value ± standard deviation.

Table 3. Thermodynamics and kinetics data for the complexation reactions of desferrioxamine B [denoted $(DFO\text{-}B)^{3-}$] and acetohydroxamate (denoted aA^-) in aqueous solution.

Reaction	log K	log k_f	log k_b
$H_3(HDFO\text{-}B)^+ = H_2(HDFO\text{-}B)^0 + H^+$	-8.51^a	—	—
$H_2(HDFO\text{-}B)^0 = H(HDFO\text{-}B)^- + H^+$	-8.73^a	—	—
$H(HDFO\text{-}B)^- = (HDFO\text{-}B)^{2-} + H^+$	-8.99^a	—	—
$(HDFO\text{-}B)^{2-} = (DFO\text{-}B)^{3-} + H^+$	-10.01^a	—	—
$H_3(HDFO\text{-}B)^+ + Fe^{3+} \overset{k_f}{\underset{k_b}{\Leftrightarrow}} FeH_2(HDFO\text{-}B)^{3+} + H^+$	3.60^b	0.30	-3.30
$FeH_2(HDFO\text{-}B)^{3+} \Leftrightarrow FeH(HDFO\text{-}B)^{2+} + H^+$	-0.72^b	-1.36	-0.64
$FeH(HDFO\text{-}B)^{2+} \Leftrightarrow Fe(HDFO\text{-}B)^+ + H^+$	-0.58^b	2.00	2.58
$aHA^0 = aA^- + H^+$	-8.89^c	—	—
$aHA^0 + Fe^{3+} \overset{k_f}{\underset{k_b}{\Leftrightarrow}} FeaA^{2+} + H^+$	1.90^c	0.62	-1.12
$FeaA^{2+} + aHA^0 \Leftrightarrow Fe(aA)_2^+ + H^+$	-0.18^c	3.16	3.34
$Fe(aA)_2^+ + aHA^0 \Leftrightarrow Fe(aH)_3^0 + H^+$	-1.79^c	3.18	4.97

^{a} Thermodynamics data at 298 K from Borgias et al. (1989). The H enclosed in parentheses is that on the amine group of the siderophore. The other H are on the hydroxamate groups (Fig. 1).

^{b} Conditional equilibrium constant and kinetics data at 298 K and 2 M ionic strength, from Biruš et al. (1987). Units of k_f are $M^{-1}\,s^{-1}$ (row 5) or s^{-1} (rows 6 and 7). Units of k_b are $M^{-1}\,s^{-1}$. k_f and k_b are forward and backward rate coefficients, respectively.

^{c} Conditional equilibrium constant and kinetics data at 298 K and 2 M ionic strength, from Biruš et al. (1985). Units of k_f and k_b are $M^{-1}\,s^{-1}$. Ionic strength is 1 M for the reaction in row 8.

Holmén and Casey (1996) have outlined a mechanism for goethite dissolution promoted by the monohydroxamate ligand, aHA. Noting that both hydrophobicity and significant conformational changes attend the surface complexation reactions of large biomolecules, such as DFO-B, Holmén and Casey (1996) speculated that only one or two hydroxamate groups in the siderophore might be able to coordinate to reactive Fe(III) centers at the mineral surface. Indeed, the general concordance, noted above, among the pseudo–first-order rate coefficients for goethite dissolution measured at 25°C in the presence of aHA, DFO-B, and DFO-D1 suggests that coordination of just one Fe(III) center at the mineral surface by the siderophores may be occurring.

This hypothesis can be examined in the light of available estimates of thermodynamic and kinetics data for the complexation of Fe^{3+} in aqueous solution by DFO-B and aHA, some of which are compiled in Table 3. Coordination of Fe^{3+} by the hydroxamate group farthest from the protonated amine in DFO-B (Fig. 1) is highly favored over subsequent coordination by a second or third hydroxamate group closer to the positive charge site (row 5 vs. rows 6 and 7 in Table 3). Indeed, the log K data (column 2) indicate an increase in the standard Gibbs energy change for the complexation reaction as a result of coordination to more than one hydroxamate group, with a concomitant increase in the kinetic lability of the complex formed (i.e., increasing k_b, column 4). The same trend is observed for the coordination of more than one aHA ligand to Fe^{3+} (row 9 vs. rows 10 and 11 in Table 3). Therefore, in aqueous solution, coordination of Fe^{3+} by a single hydroxamate group is a favored process, even though the siderophore complex involves hexadentate ligation with three hydroxamate groups (Crumbliss, 1991).

One possible cause of the more facile proton-assisted removal of hydroxamate groups in Fe-aA complexes as compared with Fe–DFO-B complexes (i.e., the larger k_b values for the Fe-aA complexes in column 4 of Table 3 as compared with

the Fe–DFO-B complexes) is the hydrophobic backbone in DFO-B (Fig. 1), which could prevent easy access of the proton to a site of Fe^{3+} coordination (Biruš et al., 1987). Another possible cause of the difference in complex stability between the siderophore and the simple hydroxamate ligand is the difference in substituent on the N atom in the coordinating hydroxamate (i.e., an alkyl group vs. a proton), which places additional electron density on the carbonyl O in the case of the siderophore (Crumbliss, 1991). These effects notwithstanding, a strong consensus exists in the literature for similarity in the complexation of Fe^{3+} by DFO-B and simple monohydroxamates (Biruš et al., 1988; Crumbliss, 1991). We believe that this consensus lends support to the hypothesis that DFO-B adsorbs on the goethite surface by use of a single hydroxamate group, as described by Holmén and Casey (1996) for aHA (their fig. 11). The same reasoning would apply to DFO-D1.

Indirect evidence for a surface complexation mechanism involving a single hydroxamate group can be adduced through an analysis of the temperature dependence of the mass-normalized dissolution rate coefficients in Table 1 via the Arrhenius equation (Lasaga, 1998),

$$k = A \exp(-E_a/RT) \qquad (1)$$

where A is a preexponential factor, E_a is an apparent activation energy, R is the gas constant, and T is absolute temperature. Lasaga (1998) has discussed the application of Eqn. 1 to rate coefficients for the proton-promoted dissolution of a wide variety of minerals. He notes that the parameters A and E_a reported for many minerals are positively correlated according to a "compensation law,"

$$\ln A = a + \alpha (E_a/R) \qquad (2)$$

where a is a parameter whose value depends on the units in which k in Eqn. 1 is expressed and α is a parameter expressing

Table 4. Adjustable parameter values for the Arrhenius equation with a compensation law (Eqn. 3)[a]

Siderophore	T (K)	α (10^{-3} K^{-1})	E_a (kJ/mol)
DFO-B	298	2.27	28.5
DFO-B	313	2.27	28.5
DFO-B	328	2.60	28.5
DFO-D1	298	2.27	21.7
DFO-D1	313	2.27	21.7
DFO-D1	328	2.42	21.7

[a] The value of the parameter a in Eqn. 3 is 1.72 for both siderophores at all three temperatures.

the positive correlation. With this relationship between A and E_a, Eqn. 1 takes the form

$$k = \exp(a) \exp\left[\left(\alpha - \frac{1}{T}\right)\frac{E_a}{R}\right] \qquad (3)$$

Lasaga (1998) has discussed Eqn. 2 in the context of the transition state theory of reaction rates, noting that a positive linear correlation between the entropy and the enthalpy of activation is implied by Eqn. 2, such that increases in E_a ("barrier height") are compensated by increases in A ("frequency factor"). If the two thermodynamic parameters obey the linear relationship,

$$\Delta S^{\ddagger} = \alpha \, \Delta H^{\ddagger} + \beta \qquad (4)$$

where S is entropy and H is enthalpy, then A and E_a are correspondingly related by the equation (Lasaga, 1998),

$$\ln A = \text{constant} + \alpha \, (E_a/R) \qquad (5)$$

which is identical in form to the compensation law in Eqn. 2. The meaning of α is the same in each expression. However, Laidler (1987) cautions against a strictly kinetics interpretation of the parameter α in Eqn. 4 because "compensation" between $\Delta S^{\ddagger}$ and $\Delta H^{\ddagger}$ is also expected solely from solvent interactions with the reactants that combine to form the activated complex. For example, if $\Delta H^{\ddagger}$ decreases because of strong solvent interactions, so will $\Delta S^{\ddagger}$ in reflecting the loss of motional freedom of solvating water molecules.

An application of Eqn. 3 is reported in Table 4. The values of the parameters a, α, and E_a were first determined by applying Eqns. 1 and 2 at 25 and 40°C. Then only the parameter α was adjusted to fit the data at 55°C while the values of a and E_a remained fixed. This procedure, followed solely for the sake of simplicity, gave values of the three adjustable parameters that yielded an excellent fit of the Arrhenius equation to the mass-normalized rate coefficient data in Table 1. Note that the prefactor, exp(a), turned out to have the same value (5.6 μmol/g/h) for both siderophores, but the apparent activation energy is somewhat larger for DFO-B than DFO-D1, as expected because of repulsion between the goethite surface and the former siderophore. The parameter α turned out to be the same for both siderophores at 25 and 40°C, but increased somewhat for both at 55°C. The two values of E_a in Table 4 are much smaller than those reported for the proton-promoted dissolution of goethite and other minerals (Wieland et al., 1988; Casey and Sposito, 1992; Cornell and Schwertmann, 1996; Lasaga, 1998).

Biruš et al. (1988) have shown that the compensation law in Eqn. 4 applies to the activation thermodynamics parameters for the reaction in which Fe^{3+} coordinates to a single hydroxamate group, either in DFO-B or in a variety of monohydroxamates. Their "isokinetic plot" (Fig. 1B in their article) can be modeled by the explicit mathematical form

$$\Delta S^{\ddagger} = 2.74 \times 10^{-3} \, \Delta H^{\ddagger} - 206 \qquad (6)$$

with $\Delta S^{\ddagger}$ in units of J/mol/K and $\Delta H^{\ddagger}$ in units of J/mol. There is a striking similarity between the coefficient of $\Delta H^{\ddagger}$ in Eqn. 6 and the values of α listed in Table 4. Biruš et al. (1988) concluded from the conformity of both DFO-B and monohydroxamate ligands to the same relation between $\Delta S^{\ddagger}$ and $\Delta H^{\ddagger}$ that a common reaction mechanism exists among these compounds in their coordination to Fe^{3+} in aqueous solution. The close correspondence of the values of α in Eqn. 6 and Table 4 leads us to speculate that DFO-B and aHA also may dissolve goethite by similar mechanisms. As noted by Holmén and Casey (1996) and seconded by Kalinowski et al. (2000), this mechanism, surprisingly, is not particularly effective at releasing Fe from goethite when compared with other common biologic ligands, such as oxalate.

REFERENCES

Albrecht-Gary A.-M. and Crumbliss A. L. (1998) Coordination chemistry of siderophores: Thermodynamics and kinetics of iron chelation and release. *Metal Ions Biol. Sys.* **35,** 239–237.

Biruš M., Bradić Z., Kujundžić N., Pribanić M., Wilkins P. C., and Wilkins R. G. (1985) Stopped-flow and rapid-scan spectral examination of the iron(III)-acethydroxamic acid system. *Inorg. Chem.* **24,** 2980–2983.

Biruš M., Bradić Z., Krznarić G., Kujundžić N., Pribanić M., Wilkins P. C., and Wilkins R. G. (1987) Kinetics of stepwise hydrolysis of ferrioxamine B and formation of diferrioxamine B in acid perchlorate solution. *Inorg. Chem.* **26,** 1000–1005.

Biruš M., Krznarić G., Kujundžaić N., and Pribanić M. (1988) Kinetic and equilibrium thermodynamic description of the interaction of desferrioxamine B and acethydroxamic acid with iron(III) in acid aqueous perchlorate. *Croat. Chem. Acta* **61,** 33–39.

Borgias B., Hugi A. D., and Raymond K. N. (1989) Isomerization and solution structures of desferrioxamine B complexes of Al^{3+} and Ga^{3+}. *Inorg. Chem.* **28,** 3538–3545.

Brantley S. L. and Chen Y. (1995) Chemical weathering rates of pyroxenes and amphiboles. *Rev. Mineral.* **31,** 119–172.

Casey W. H. and Sposito G. (1992) On the temperature dependence of mineral dissolution rates. *Geochim. Cosmochim. Acta* **56,** 3825–3830.

Cornell R. M. and Schwertmann U. (1996) *The Iron Oxides.* VCH.

Crumbliss A. (1991) Aqueous solution equilibrium and kinetic studies of iron siderophore and model siderophore complexes. In *Handbook of Microbial Iron Chelates* (ed. G. Winkelmann), pp. 177–232. CRC Press.

Eick M. J., Peak J. D., and Brady W. D. (1999) The effect of oxyanions

on the oxalate-promoted dissolution of goethite. *Soil Sci. Soc. Am. J.* **63,** 1133–1141.

Holmén B. A. and Casey W. H. (1996) Hydroxamate ligands, surface chemistry, and the mechanism of ligand-promoted dissolution of goethite [α-FeOOH(s)]. *Geochim. Cosmochim. Acta* **60,** 4403–4416.

Holmén B. A., Tejedor-Tejedor M. I., and Casey W. H. (1997) Hydroxamate complexes in solution and at the goethite–water interface: A cylindrical internal reflection Fourier transform infrared spectroscopy study. *Langmuir* **13,** 2197–2206.

Holmén B. A. and Casey W. H. (1998) Erratum to Hydroxamate ligands, surface chemistry, and the mechanism of ligand-promoted dissolution of goethite [α-FeOOH(s)]. *Geochim. Cosmochim. Acta* **62,** 726.

Kalinowski B. E., Liermann L. J., Givens S., and Brantley S. L. (2000) Rates of bacteria-promoted solubilization of Fe from minerals: A review of problems and approaches. *Chem. Geol.* **169,** 357–370.

Kraemer S. M., Cheah S.-F., Zapf R., Xu J., Raymond K., and Sposito G. (1999) Effect of hydroxamate siderophores on Fe release and Pb(II) adsorption by goethite. *Geochem. Cosmochem. Acta* **63,** 3003–3008.

Laidler K. J. (1987) *Chemical Kinetics.* Harper and Row.

Lasaga A. C. (1998) *Kinetic Theory in the Earth Sciences.* Princeton University Press.

Liermann L. J., Kalinowski B. E., Brantley S. L., and Ferry J. G. (2000) Role of bacterial siderophores in dissolution of hornblende. *Geochim. Cosmochim. Acta* **64,** 587–602.

Rodda D. P., Johnson B. B., and Wells J. D. (1993) The effect of temperature and pH on the adsorption of copper(I), lead(II), and zinc(II) onto goethite. *J. Colloid Interface Sci.* **161,** 57–62.

Schwertmann U. and Cornell R. M. (1991) *Iron Oxides in the Laboratory.* VCH.

Solinas V. (1994) Cation effects on the adsorption of deferrioxamine B (DFOB) by humic acid. In *Humic Substances in the Global Environment and Implications on Human Health* (eds. N. Senesi and T. M. Miano), pp. 1183–1188. Elsevier Science.

Sposito G. (1994) *Chemical Equilibria and Kinetics in Soils.* Oxford University Press.

Stumm W. and Furrer G. (1987) The dissolution of oxides and aluminum silicates; examples of surface-controlled kinetics. In *Aquatic Surface Chemistry* (ed. W. Stumm), pp. 197–219. Wiley-Interscience.

Stumm W., Wehrli B., and Wieland E. (1987) Surface complexation and its impact on geochemical kinetics. *Croat. Chem. Acta* **50,** 1861–1869.

van der Helm D., Jalal M. A. F., and Hossain M. B. (1987) The crystal structures, conformations, and configurations of siderophores. In *Iron Transport in Microbes, Plants and Animals* (eds. G. Winkelmann, D. van der Helm, and J. B. Neilands), pp. 135–165. VCH.

Wieland E., Wehrli B., and Stumm W. (1988) The coordination chemistry of weathering: III. A generalization on the dissolution rates of minerals. *Geochim. Cosmochim. Acta* **52,** 1969–1981.

Yu Q., Kandegedara A., Xu Y., and Rorabacher D. B. (1997) Avoiding interferences from Good's buffers: A contiguous series of noncomplexing tertiary amine buffers covering the entire range of pH 3–11. *Anal. Biochem.* **253,** 50–56.

Zinder B, Furrer G., and Stumm W. (1986) The coordination chemistry of weathering: II. Dissolution of Fe(III) oxides. *Geochim. Cosmochim. Acta* **50,** 1861–1869.